Article

Optically Activated Functionalization Reactions in Si Quantum Dots

Fernando A. Reboredo, Eric Schwegler, and Giulia Galli

More About This Article

Additional resources and features associated with this article are available within the HTML version:

- Supporting Information
- Access to high resolution figures
- Links to articles and content related to this article
- Copyright permission to reproduce figures and/or text from this article

View the Full Text HTML

Optically Activated Functionalization Reactions in Si Quantum Dots

Fernando A. Reboredo,* Eric Schwegler, and Giulia Galli

Contribution from the Lawrence Livermore National Laboratory, Livermore, California 94588

Received March 20, 2003; E-mail: reboredo1@llnl.gov

Abstract: Using ab initio calculations, we have studied the influence of optical activation on functionalization reactions of silicon quantum dots with unsaturated hydrocarbons. We find that the energy barrier for the replacement of silicon−hydrogen with silicon−carbon bonds is dramatically reduced if the silicon dot is optically excited. These results provide an explanation for recent experiments on optically excited porous silicon. In addition, our calculations point at the existence of an intermediate spin-polarized state formed by the dot and an alkene or alkyne, upon relaxation after absorbing a photon. This state could be detected experimentally, by, for example, electron spin resonance measurements. Based on the results of our calculations as a function of the dot size, varied from 0.8 to 1.5 nm, we propose that light activated reactions could be used to functionalize and size select silicon quantum dots at the same time.

1. Introduction

Silicon surface chemistry is of fundamental importance because of the ubiquitous role of silicon in modern technology. In particular, enabling direct electronic interfaces of organic molecules with silicon architectures, for example, porous silicon and Si quantum dots (QD), is a key step for the design of optoelectronic devices and biosensors.[1] For these applications, a patterned surface is required, to connect molecular switches or to locate biological or chemical species on a substrate that exhibits their preferred texture.[2,3] While selective absorption on Si surfaces has been achieved at the micrometer scale, it becomes much more challenging to perform at the nanoscale.

Although a variety of syntheses of Si nanoparticles and quantum dots (QD) have appeared in the recent literature,[4,5] most of the progress in functionalizing Si surfaces at the nanoscale has been achieved with porous Si (p-Si),[6] which is a material relatively easy to produce and exhibits bright, tunable, room-temperature photoluminescence. Porous silicon has a complex, nanoscale architecture, and quantum confinement effects of the embedded nanoparticles are believed to be responsible for its visible photoluminescence.

Unlike the case of bulk Si surfaces,[7] where H atoms and other contaminants can be removed by temperature annealing before the surface is functionalized, in p-Si and Si QD, a hydride-terminated interface is utilized. As a result, the reaction involves both cleavage of a Si−H bond, and formation of a new Si−C bond along the reaction pathway. Nanoscale Si with organic terminated surfaces can be obtained from a wide variety of methods.[6] In particular, a novel method has been recently proposed,[2] which is based on a white light promoted hydro-silylation reaction enabling the functionalization of p-Si with unsaturated organic molecules. This reaction appears to be directly related to quantum confinement effects and has no counterpart in the chemistry of bulk Si surfaces. The technique proposed in ref 2 is particularly promising, since it may enable selectivity in the functionalization of different regions of a p-Si sample, using optical masking techniques. Experimental evidence suggests that these white light activated reactions are mediated by the formation of an exciton in the confined Si structure, which may live long enough to drastically change the excited-state chemistry compared to ground-state processes.

Theoretical work on optically activated reactions in Si QD or p-Si has been very limited. The nature of the problem calls for a quantum mechanical treatment of chemical reactions in the ground and excited states, and the need to obtain predictive results calls for the use of ab initio methods. These are computationally very demanding and no investigation of the attachment of hydrocarbons to Si QD using first principles techniques has yet appeared in the literature. However, an early ab initio calculation pointed at the importance of electronic excitations in Si-QD. In particular, Allan et al.[8] showed that the presence of an exciton in Si-QD significantly reduces the energy barrier required to open a dimer on the surface.

In this work, we present a first principles investigation of the mechanism leading to optically activated hydrosilylation of Si dots with alkenyl and alkanyl groups. In particular, we present

(1) Schmedake, T. A.; F. Cunin, F.; Link, J. R.; Sailor, M. J. *Adv. Mater.* **2002**, *14*, 1270−1272 and references therein. Sohn, H.; Létant, S.; Sailor, J. M.; Trogler, W. C. *J. Am. Chem. Soc.* **2000**, *122*, 5399−5400. Dancil, K.-P. S.; Greiner, D. P.; Sailor, M. J. *J. Am. Chem. Soc.* **1999**, *121*, 7925−7930.
(2) Stewart, M. P.; Buriak, J. M. *J. Am. Chem. Soc.* **2001**, *123*, 7821−7830.
(3) Bruchez, M.; Moronne, M.; Gin, P.; Weiss, S.; Alivisatos, A. P. *Science* **1998**, *281*, 2013−2016. Chan, W. C. W.; Nie, S. M. *Science* **1998**, *281*, 2016−2018.
(4) Baldwin, R. K.; Pettigrew, K. A.; Garno, J. C.; Power, P. P.; Liu, G.-Y.; Kauzlarich, S. M. *J. Am. Chem. Soc.* **2002**, *124*, 1150−1151.
(5) Holmes, J. D.; Ziegler, K. J.; Doty, R. C.; Pell, L. E.; Johnston, K. P.; Korgel, B. A. *J. Am. Chem. Soc.* **2001**, *123*, 3743−3748.
(6) Stewart, M. P.; Buriak, J. M. *Comments Inorg. Chem.* **2002**, *23*, 179−203.
(7) Bent, S. F. *Surf. Sci.* **2002**, *500*, 879−903.

(8) Allan, G.; Delerue, C.; Lannoo, M. *Phys. Rev. Lett.* **1996**, *76*, 2961−2964.

results of density functional calculations showing that energy barriers between a Si-QD and C_2H_2 and C_2H_4 molecules are dramatically different if the dot is in its ground state or it is optically excited. When the dot is excited to the lowest energy triplet state, we find that the reaction between the dot and C_2H_2 or C_2H_4 leads to the formation of an intermediate metastable state, where the triplet spin configuration is the electronic ground state. In this intermediate configuration, a silicon atom forms a bond with one of the unsaturated C atoms and becomes 5-fold coordinated. The π-type character of bonding in the unsaturated carbon chain plays a crucial role in the formation of the intermediate state. Based on our results, we propose a method to "gap select" Si quantum dots as the same time as they are functionalized with specific surfactants.

2. Method

We computed formation energies and energy barriers using density functional theory (DFT) in the generalized gradient approximation (GGA) proposed by Perdew et al.[9] (PBE) and treating spin variables explicitly. The ground- and excited-state configurations of Si dots were obtained by forcing the total spin to be $S = 0$ or the projection of the total spin to be $S_z = 1$, respectively.[10] Most of our calculations were performed using a plane-wave pseudopotential method and were carried out with the GP code.[11] The Si and C pseudopotentials were generated with the Troullier−Martins prescription,[12] and a kinetic energy cutoff of 35 and 140 Ry was used to represent the single particle wave functions and charge density, respectively. We modeled most of the reactions of silicon quantum dots and unsaturated carbon chains with a cluster of $Si_{29}H_{24}$ in the presence of an ethene or ethyne molecule. Reaction barriers involving ethene were also calculated using $Si_{66}H_{40}$ and $Si_{142}H_{72}$ clusters but, in the latter case, only in the local density approximation (LDA). The dot and molecules were placed in a periodically repeated supercell, with the nearest distance between atoms in different supercells being larger than 16 Å.[13] Geometry relaxations were performed until forces acting on all atoms were smaller than 10^{-4} atomic units. To test the sensitivity of our results to the choice of the exchange correlation functional, we repeated some of our calculations using the hybrid B3LYP functional[14] and a code[15] using Gaussian basis sets.

The electronic configuration of a fully passivated semiconductor QD in the ground state is a singlet (total spin $S = 0$) and the first excited state is a triplet ($S = 1$). In this *particular* case, where the spin symmetries of the first excited and ground state are different, the excitation energy of the dot can be defined as the difference between the total energies of the two configurations, as computed within spin density functional theory (SDFT).[10] Although this excitation energy

may not be directly comparable to an experimentally determined exciton energy (given the approximations adopted here for the exchange-energy functional), we will assume throughout this work that the computed excitation energies represent a qualitatively meaningful estimate of the dot exciton energies. Alternatively, one could have obtained exciton energies from quasi particle gaps, after subtracting an estimate of the electron−hole binding energy.[16] However, questions concerning the gap error correction and the way electron−hole polarization energies are evaluated[16] are still subjects of controversy,[17] and these energies have not been estimated in this work.

2.1. Calculation of the Energy Barriers. Transition-state theory (TST, ref 18 and references therein) is based on the assumption that transition rates can be evaluated by computing total energies at extrema along a minimum-energy path (MEP), as well as curvatures of the total, ground-state energy surface at these extrema. As long as the energy differences between different energy paths are much larger than kT, dynamical excitation effects can be neglected, at least qualitatively. Including dynamical excitations beyond TST within a first principles description would be extremely difficult, and to date, there are no methods available to do so for the size of systems considered here.

Our calculations of energy barriers involve a large number of atoms, a large number of basis functions, and different magnetic configurations; therefore, we chose to compute transition-state energies and positions using a method which requires the storange of only one copy of the atomic and electronic coordinates at a time. We devised an algorithm based on the assumption that a transition-state configuration can be found using a small number of degrees of freedom to define the transition path. This algorithm turns out to be a combination of one of the simplest (drag method[18]) and one of the most computationally demanding (Hessian method[19]) approaches proposed in the literature to compute transition states.

The drag method[18] consists of constraining one degree of freedom (e.g., distance, angle, etc.). This defines a so-called constraint surface. The constraint coordinate follows a pre-established path while allowing the rest of the system to relax to the closest local minimum configuration. The main disadvantage of the drag method is the arbitrary choice of a reaction coordinate, which may not lead to the most energetically favorable transition state.

In Hessian based methods,[19] an ionic configuration $\{R\}$ is first selected, which is reasonably close to a transition point. Subsequently, one evaluates the Hessian matrix $\mathbf{H}_M$ formed by the second derivatives of the total energy with respect to the atomic displacements. The curvature of the potential energy surface at $\{R\}$ is given by $^1/_2\{\Delta R\}\cdot\mathbf{H}_M\cdot\{\Delta R\}$, where $\{\Delta R\}$ is the vector of atomic displacements from $\{R\}$. The transition state is searched by moving the system "up hill" along the direction of minimum curvature, or reaction coordinate $\mathbf{d}_{RC}$ (which corresponds to the eigenvector of the smallest eigenvalue of $\mathbf{H}_M$), while minimizing the forces along all other directions. A big disadvantage of the Hessian method is the computational cost involved in the calculation of $\mathbf{H}_M$ for large systems.

In our combined approach, we use an estimate of $\mathbf{d}_{RC}$ to define an appropriate reaction coordinate. In the vicinity of a transition-state configuration ($\{R\}_T$), the Kohn−Sham energy $E_{KS}(\{R\})$ can be written in the basis of the eigenvectors of $\mathbf{H}_M$ as $E_{KS}(\{R\}_T) + {}^1/_2(\sum_{i\neq j} k_i d\rho_i^2 + k_j d\rho_j^2)$, where the κ_i (κ_j) are the positive (negative) eigenvalues of the Hessian matrix (corresponding to $\mathbf{d}_{RC}$) and ρ_i are the projections of $\{\Delta R\}$ on the eigenvectors of $\mathbf{H}_M$ (i.e., $d\rho_j = \{\Delta R\}\cdot\mathbf{d}_{RC}$). For the drag method to work, $\{R\}_T$ must be a minimum of $E_{KS}(\{R\})$ among the

(9) Perdew, J. P.; Burke, K.; Ernzerholf, M. *Phys. Rev. Lett.* **1996**, *77*, 3865−3868.

(10) Gunnarsson, O.; Lundqvist, B. L. *Phys. Rev. B* **1976**, *13*, 4274. Parr, R. G.; Yang, W. *Density-Functional Theory of Atoms and Molecules;* Oxford University Press: New York, 1989; p 205.

(11) Most of our DFT calculations were carried out using a parallel first principles molecular dynamics general pourpose code, GP 1.14.1 (F. Gygi, LLNL 1999−2001).

(12) Troullier, N.; Martins, J. L. *Phys. Rev. B* **1991**, *43*, 1993−2006.

(13) This was necessary to avoid possible dipole−dipole interactions of polarized bonds as well as to avoid quantum overlap between neighboring supercells.

(14) Becke, A. D. *J. Chem. Phys.* **1993**, *98*, 5648−5652.

(15) Frisch, M. J.; Trucks, G. W.; Schlegel, H. B.; Scuseria, G. E.; Robb, M. A.; Cheeseman, J. R.; Zakrzewski, V. G.; Montgomery, J. A., Jr.; Stratmann, R. E.; Burant, J. C.; Dapprich, S.; Millam, J. M.; Daniels, A. D.; Kudin, K. N.; Strain, M. C.; Farkas, O.; Tomasi, J.; Barone, V.; Cossi, M.; Cammi, R.; Mennucci, B.; Pomelli, C.; Adamo, C.; Clifford, S.; Ochterski, J.; Petersson, G. A.; Ayala, P. Y.; Cui, Q.; Morokuma, K.; Malick, D. K.; Rabuck, A. D.; Raghavachari, K.; Foresman, J. B.; Cioslowski, J.; Ortiz, J. V.; Baboul, A. G.; Stefanov, B. B.; Liu, G.; Liashenko, A.; Piskorz, P.; Komaromi, I.; Gomperts, R.; Martin, R. L.; Fox, D. J.; Keith, T.; Al-Laham, M. A.; Peng, C. Y.; Nanayakkara, A.; Gonzalez, C.; Challacombe, M.; Gill, P. M. W.; Johnson, B.; Chen, W.; Wong, M. W.; Andres, J. L.; Gonzalez, C.; Head-Gordon, M.; Replogle, E. S.; Pople, J. A. *Gaussian 98*, revision A.7; Gaussian Inc.: Pittsburgh, PA, 1998.

(16) Öğüt, S.; Chelikowsky J.; Louie, S. *Phys. Rev. Lett.* **1997**, *79*, 1770−1773.

(17) Godby, R. W.; White, I. D. *Phys. Rev. Lett.* **1998**, *80*, 3161. Franceschetti, A.; Wang, L. W.; Zunger, A. *Phys. Rev. Lett.* **1999**, *83*, 1269.

(18) Henkelman, G.; Jóhannesson, G.; Jónsson, H. In *Theoretical Methods in Condensed Phase Chemistry;* Schwartz, S. D., Ed.; Progress on Theoretical Chemistry and Physics; Kluwer Academic Publishers: New York, NY, 2000.

(19) Jensen, F. *Introduction to Computational Chemistry*; John Willey & Sons: Chichester, U.K., 1999; Section 14.5.9.

$\{R\}$ that belong to the same constraint surface. In the vicinity of $\{R\}_T$, the constraint surface can be approximated by the plane $\mathbf{n}_\lambda \cdot \{\Delta R\} = \lambda$, where $\mathbf{n}_\lambda$ is perpendicular to the constraint surface and $\lambda = 0$ when $\{R\}_T$ belongs to the surface. Requiring that $\{\Delta R\} = 0$ be a minimum of $(\sum_{i \neq j} k_i d\rho_i^2 + k_j d\rho_j^2)$ under the condition $\mathbf{n}_\lambda \cdot \{\Delta R\} = 0$ implies that $\mathbf{n}_\lambda$ must satisfy the condition

$$\sum_{i \neq j} \frac{\kappa_j}{\kappa_i} \nu_i^2 + \nu_j^2 > 0 \tag{1}$$

where the ν_i are the projections of $\mathbf{n}_\lambda$ in the orthonormal basis of eigenvectors of $\mathbf{H}_M$. Since κ_j is negative, eq 1 is satisfied if $|\mathbf{n}_\lambda \mathbf{d}_{RC}| = |\nu_j|$ is large. Therefore, the accuracy required to estimate the constraint in the drag method depends on the curvature of $E_{KS}(\{R\})$. It can be easily shown that if eq 1 is satisfied, $E_{KS}(\lambda)$ is approximately a parabola (obtaining the same values independently of the sign of the increment of λ).

To find an approximate position of the transition point and then find a constraint satisfying eq 1, we proceed as follows:

(1) We identify the distances $d_{i,j}$ corresponding to the bonds that are expected to break and to those that are expected to form and define a constraint surface:

$$\sum_{i \neq j} \alpha_{i,j} d_{i,j} = \lambda \tag{2}$$

(2) Different transition points are found for different values of $\alpha_{i,j}$. To drive the system into the reactions of interest, we use negative $\alpha_{i,j}$ for the bonds that will be *formed* and positive $\alpha_{i,j}$ for the ones that will be *broken*. While several choices of $\alpha_{i,j}$ must be tried, it is often useful to set the absolute values roughly proportional to the corresponding bond spring constants obtained numerically.

(3) The initial value of λ is chosen so that eq 2 is satisfied in the initial reactant structure and then λ is increased periodically while relaxing the forces in all the remaining degrees of freedom at every step. $E_{KS}(\lambda)$ is the minimum Kohn–Sham energy consistent with the constraint in eq 2. $E_{KS}(\lambda)$ is obtained using a Lagrange multiplier method. The proximity to a transition point is identified when the second derivative of $E_{KS}(\lambda)$ becomes negative.

(4) Having identified a region of negative curvature, we optimize the constraint as follows: We evaluate a reduced Hessian matrix $\mathbf{H}_R$ which is a second-order expansion of the $E_{KS}(\{R\})$ but only for the degrees of freedom involved in eq 2. $\mathbf{H}_R$ is evaluated numerically using a finite difference method *fully relaxing the remaining degrees of freedom of the system* for each finite displacement. The set of $\alpha_{i,j}$ is changed in such a way to make the surface defined by eq 2 perpendicular to the eigenvector corresponding to the negative eigenvalue of $\mathbf{H}_R$ [which maximizes the value of ν_j^2 in eq 1].

(5) Finally, we identify a transition state when an inverted parabola is found at the maximum of $E_{KS}(\lambda)$ independently of the sign of the increment of λ. If instead, a sudden drop of $E_{KS}(\lambda)$ to another branch is found, one can estimate an upper bound and lower bound for the transition-state energy. The lower bound is the energy where the two solutions of $E_{KS}(\lambda)$ cross as a function of λ while the upper bound is the lowest maximum before the drop.

(6) If the estimate of the transition state obtained in step 5 is not satisfactory, we refine the constraint as follows: We identify the distance [not included in eq 2] that suffers the largest change when the two solutions of $E_{KS}(\lambda)$ cross. We add this distance to the ones considered in eq 2, and we re-evaluate $\mathbf{H}_R$ at the middle point (between the configurations $\{R\}$ corresponding to the two solutions of $E_{KS}(\lambda)$ at the crossing point). Once a new constraint with this additional distance is defined from $\mathbf{H}_R$, the process is repeated until a well behaved parabola is found or a sufficiently narrow estimate is reached.

In the cases studied here, up to five distances were included in eq 2. Transition points in the energy barriers were refined until the

maximum force on the constraint atoms was 8×10^{-4} atomic units while forces on the remaining degrees of freedom were all lower than 10^{-4} atomic units.

If the constraint optimization step is omitted, we are left with the drag method. On the other hand, if $3(N - 2) + 1$ independent internal coordinates are considered in eq 1 and if the constraint is optimized at every step, our method for transition-state search reduces to a Hessian based method. Therefore, as most local methods in the literature, this method will be numerically unstable if more than one eigenvalue of the Hessian matrix is close to zero or negative in the vicinity of the transition point. Ultimately, the transition point found by this algorithm is biased by the initial guess for the $\alpha_{i,j}$. Because we are dealing with a large number of atoms, there is always the possibility for some unexpected reaction path providing a lower energy transition state. Thus several choices for the $\alpha_{i,j}$ must be tested until one is reasonably convinced that the transition point found is a representative estimate of the energy barrier of the process of interest.

3. Results

3.1. Description of the Model System. We have chosen $Si_{29}H_{24}$ as a model system to study hydrosilylation reactions with ethene (C_2H_4) and ethyne (C_2H_2) molecules because the surface properties of this cluster have been studied by several groups[8,20−22] and thus its structure is fairly well understood. $Si_{29}H_{24}$ has 24 surface Si atoms, which are monohydrides, and five Si atoms in the core, which are only bonded to other Si atoms. There are two types of surface Si atoms, 12 of them belong to (111) like facets, and 12 form six dimers analogous to those found on (100), (2×1) reconstructed hydrogenated flat surfaces.[23] We note that a Si_{29} cluster can be fully hydrogenated to give $Si_{29}H_{36}$ for very high values of the H chemical potential. This would correspond to an environment where C_2H_4 could transform to C_2H_6 (an alkane with far less chemical reactivity). It is thus reasonable to expect that reactions with unsaturated hydrocarbons are more likely to occur with the lowest H content Si clusters, that is, $Si_{29}H_{24}$, which according to our recent studies is fairly stable along a wide range of H chemical potentials.[20] We stress that in $Si_{29}H_{24}$ there are no dangling bonds available. Therefore, it is not particularly reactive, similar to the case of (2×1) hydrogenated flat (100) surfaces. For all the cluster sizes considered here, we chose a Si atom on a (111) facet as the one eventually forming a Si–C bond. We will call this atom "*the reactant* Si".

3.2. Reactions with Si Quantum Dots in the Singlet Ground State. In Figure 1, we present our results for the energy path of the reaction $Si_{29}H_{24} + C_2H_4 \rightarrow Si_{29}H_{23}–CH_2–CH_3$, when the Si dot is in the electronic ground state ($S = 0$). This reaction results in a functionalized QD where a Si–H bond on the surface has been replaced by a Si bonded to an ethanyl group ($Si–CH_2–CH_3$). According to our calculations, this reaction is exothermic and it provides 1.49 eV (1 eV = 23.061 kcal/mol). To obtain such an energy gain, the system has to overcome an energy barrier of 2.12 ± 0.02 eV[24] in a vacuum. As shown in the inset, in the transition state, the Si–H bond is broken and

(20) Puzder, A.; Williamson A. J.; Reboredo, F. A.; Galli, G. *Phys. Rev. Lett.* **2003**, *91*, 157405.
(21) Mitas, L.; Therrien, J.; Twesten, R.; Berlomoin, G.; Nayfeh, M. H. *Appl. Phys. Lett.* **2001**, *78*, 1918−1920.
(22) Vasiliev, I.; Martin, R. M. *Phys. Status Solidi B* **2002**, *233*, 5−9.
(23) Northrup, J. E. *Phys. Rev. B* **1991**, *44*, 1419−1422 and references therein.
(24) The error in the determination of the energy barriers is a result of the fact that the symmetry of the ethane molecule is broken at the transition which gives rise to a very flat energy surface at the transition point which hinders the precise determination of the energy barrier.
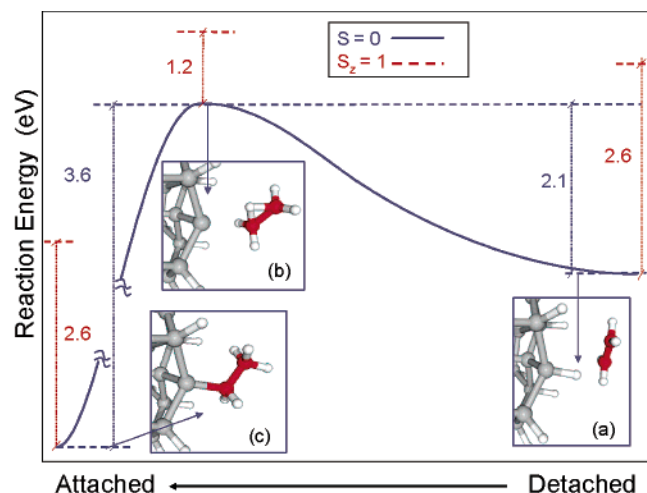
Figure 1. Schematic representation of the hydrosilylation reaction $Si_{29}H_{24} + C_2H_4 \rightarrow Si_{29}H_{23}-CH_2-CH_3$ in the singlet state ($S_z = 0$): continuous blue line. The red broken lines correspond to the energy of the triplet state ($S_z = 1$) in the geometry of the singlet configuration. The atomic configurations of the reactants, product, and transition state are given in the insets.

the H atom is shared by two C atoms before the formation of a Si−C bond occurs. Although the proximity of the C_2H_4 molecule to the dot reduces the energy required to break a Si−H bond by more than 1.4 eV (as compared to the energy required to remove an H atom from the surface in the absence of C_2H_4), this reaction still requires a considerable activation energy. Experimentally, this activation energy will seldom coincide with the simultaneous presence of an ethene molecule in the vicinity of a dot. Therefore, the rate of a hydrosilylation reaction in the singlet state of a Si dot is expected to be rather slow unless a catalyst, which is not considered in this study, is able to significantly lower the energy barrier.

In Figure 1, we also give the energies of the excited-state ($S_z = 1$) configuration calculated for the geometries of the initial, final, and transition-state geometries obtained for the ground state. The values found here suggest a strong dependence of the energy barrier between ethene and the Si dot on the excitation of the dot. Based on these results, we chose to explore the same reaction but with a dot in its first excited state ($S_z = 1$), allowing full geometrical relaxations after excitation of the dot.

3.3. Reactions with Si Quantum Dots in an Excited State. UV light is known to efficiently break Si−H bonds with resonant energy on flat bulk surfaces. The reaction discovered in ref 2, however, is activated by white light and is related to quantum confinement because it is observed only in porous silicon and is hindered by chemicals that affect the photoluminescence.

There are several reasons to argue in favor of a different chemistry if the Si dot is in an excited state. In most semiconductors, the time scale for electron−phonon interaction is much faster than that of the electron−hole recombination. Therefore, before recombination occurs (within femtoseconds), a photogenerated electron−hole pair can decay to the minimum energy configuration of the exciton, where the total spin is one (triplet state).[25] The extra energy provided to the system will contribute to the vibrational motion of the ions. However, in the case of a singlet ground state, the decay from a triplet excited state is forbidden by spin symmetry. In principle, spin−orbit

coupling and thermal excitation from the triplet state to singlet states higher in energy could make the transition possible. However, in the case of Si quantum dots, singlet-to-singlet recombination lifetimes are of the order of hundreds of nanoseconds, even for QDs as small as $Si_{29}H_{36}$.[20] In addition, these recombination times are larger in the case of clusters with reconstructed surfaces such as, for example, $Si_{29}H_{24}$.[20] For much larger Si QDs, it has been found that excitons have even longer lifetimes because the electron and the hole wave functions retain much of the indirect character of bulk silicon.[25]

3.3.1. Reactions in the Triplet State. To model the dot in an electronic excited state, we have promoted an electron from the highest occupied molecular orbital (HOMO)$\tilde{\psi}_{HOMO,\downarrow}$ as defined in the ground-state configuration of the dot into the lowest unoccupied molecular orbital (LUMO) $\tilde{\psi}_{LUMO,\uparrow}$, again as defined in the ground state. In contrast to the ground state where all single particle wave functions are doubly occupied and the total spin is $S = 0$, here the system is forced to have a different total spin symmetry $S_z = 1$. The minimum energy configuration within all possible states with $S_z = 1$ corresponds to a triplet ($S = 1$),[25] since excitations with $\Delta S > 1$ would require multiple electron−hole pairs. As mentioned in section 2, the method adopted here allows us to calculate total energies and forces for excited states according to the theorem of Gunnarsson and Lundqvist.[10] On the other hand, excited states with the same symmetry as that of the ground state ($S_z = 0$) could not be described using Gunnarson and Lunqvist's method.[10]

We note that, in the case of ground state reactions, the GGA in general gives energy barriers that are significantly improved with respect to those obtained within the LDA.[26] However, much less is known about the GGA performance in describing reactions with one of the reactants in the excited state. Here we focus on the differences between the ground and excited energy barriers; these differences are so large, as we will see, that we expect the qualitative answers provided by GGA to be correct.

Figure 2 shows the same reaction studied in Figure 1 but in the case of a dot in the excited triplet state ($S_z = 1$). We use as energy reference the product configuration ($Si_{29}H_{23}-CH_2-CH_3$) in the unpolarized ($S = 0$) ground state. Note that in order to excite $Si_{29}H_{24}$ from the geometry of the relaxed ground state one has to provide a photon with an energy of approximately 2.6 eV according to PBE-SDA. Relaxation of the forces from the ground-state geometry lowers the energy by about 0.45 eV [compare Figures 1a and 2a], which can contribute to the kinetic energy in the ions. This extra phonon energy and the original thermal energy of the system would be available to overcome energy barriers. Interestingly, we found that when the dot is in the excited state, an *intermediate bound state* can be formed and this process does not require a significant activation energy [see Figure 1b]. The formation of this intermediate state is described below.

3.3.2. Intermediate-State Configuration. In the intermediate state found in our calculations, the reactant Si forms an additional bond with one of the C atoms in the ethene molecule, leading to an sp^3 bonded C atom [see Figure 2b]. Although 5-fold coordinated Si atoms are not as energetically favored as

(25) Reboredo, F. A.; Franceschetti, A.; Zunger, A. *Phys. Rev. B* **2000**, *61*, 13073−13087.
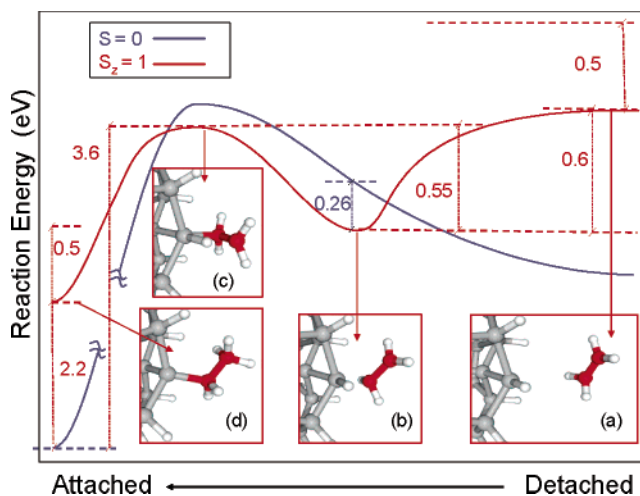(26) Grossman, J. C.; Mitas, L. *Phys. Rev. Lett.* **1997**, *79*, 4353−4356.

Figure 2. Schematic representation of the hydrosilylation reaction $Si_{29}H_{24} + C_2H_4 \rightarrow Si_{29}H_{23}-CH_2-CH_3$ in the triplet state ($S_z = 1$) state: continuous red line. The energy values for the singlet configuration reported in Figure 1 are shown again here for comparison (blue line), and the dashed red lines correspond to the energies of the excited electronic configuration ($S_z = 1$) in the relaxed geometry of the ground state ($S = 0$). Note the large Stokes shift computed for the geometry of the singlet state ($S_z = 0$). The atomic configurations of the reactants, product, and transition state are shown in the insets. Note the appearance of a metastable state (see text).

4-fold coordinates ones, 5-fold Si sites have been observed in other systems, for example, silicon interstitials in the bulk and Si defects in amorphous Si. Upon formation of the intermediate state, the interatomic distances between the 5-fold coordinated reactant Si and other Si atoms in the dot are increased. The reactant Si−H bond is significantly distorted with respect to its original (111) orientation, and its length increases from 1.51 to 1.54 Å. The reactant Si atom is back-bonded to two surface Si atoms and one core Si; the distance to the surface Si atoms increases by 4% (from 2.35 to 2.44 to Å) while the distance to the core atom increases by 10%. The geometrical distortion observed in the intermediate state is strongly concentrated around the reactant Si. The changes in all the other first neighbor distances in the Si cluster are smaller than 0.5% as compared with the unperturbed dot. The distance from the reactant Si to C is 1.95 Å (only 2% larger than the final value in $Si_{29}H_{23}-CH_2-CH_3$). As one of the C atoms in the molecule approaches the reactant Si, the distance to the other C increases by 11% (1.48 Å), becoming closer to a typical C−C single bond distance.

Surprisingly, if the atomic configuration corresponding to the intermediate state is forced to be in an unpolarized state ($S = 0$), its energy increases by 0.26 eV with respect to that in a triplet state. This means that the intermediate state found here is not only stable with respect to ionic displacements but also with respect to a spin flip. This opens the possibility to actually measure this intermediate state with, for example, electron spin resonance experiments.

As mentioned above, the geometrical distortion associated with the intermediate state is strongly localized around the reactant Si atom. We show below that in the intermediate-state electronic states are localized as well. This localization suggests that the formation energy of the intermediate state should be independent of the size of the dot.

In Figure 3a, we show a contour plot of the total spin density $\sigma(\mathbf{r}) = \rho_\uparrow(\mathbf{r}) - \rho_\downarrow(\mathbf{r})$, where $\rho_\uparrow(\mathbf{r})$ and $\rho_\downarrow(\mathbf{r})$ are the probability
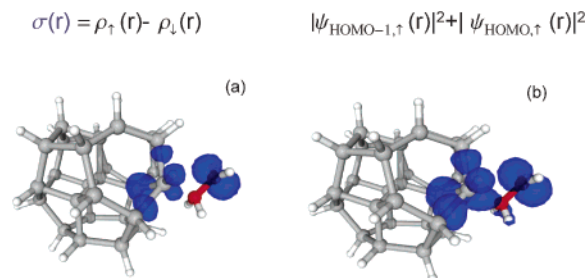
$$\sigma(r) = \rho_\uparrow(r) - \rho_\downarrow(r) \qquad |\psi_{HOMO-1,\uparrow}(r)|^2 + |\psi_{HOMO,\uparrow}(r)|^2$$

Figure 3. (a) Median isosurface of the total spin density $\sigma(r) = \rho_\uparrow(r) - \rho_\downarrow(r)$ for the intermediate state in the ($S_z = 1$) configuration [see text and Figure 2b]. (b) Median isosurface for $\frac{1}{2}(|\psi_{HOMO,\uparrow}(r)|^2 + |\psi_{HOMO-1,\uparrow}(r)|^2)$.

densities corresponding to spin up and down, respectively. The isosurface value has been chosen so that the integral within the volume enclosed by the isosurface is exactly $\frac{1}{2}$ of the total integral $\int \sigma(\mathbf{r})d\mathbf{r} = 1$. Figure 3a shows that the spin density associated with the triplet state is partly localized around the stretched bonds between the reactant Si atom and its first neighbors and partly localized in the "p" orbital of the sp^2 C atom of the former ethene molecule. We note that $\sigma(\mathbf{r})$ is almost identical to $\frac{1}{2}(|\psi_{HOMO,\uparrow}(\mathbf{r})|^2 + |\psi_{HOMO-1,\uparrow}(\mathbf{r})|^2)$ (i.e., the sum of the probability densities corresponding to the two highest occupied molecular orbitals with spin up multiplied by $\frac{1}{2}$) [see Figure 3b] indicating that the contribution to $\sigma(\mathbf{r})$ of the remaining single particle states cancels out. Both $|\psi_{HOMO,\uparrow}(\mathbf{r})|^2$ and $|\psi_{HOMO-1,\uparrow}(\mathbf{r})|$ are extended over the stretched bonds in the dot and in the "p" carbon orbital. In contrast, $|\psi_{LUMO,\downarrow}(\mathbf{r})|^2$ is strongly localized on the stretched bonds of the Si dot and has a negligible projection into the "p" orbital in the sp^2 C atom, while $|\psi_{LUMO+1,\downarrow}\mathbf{r})|^2$ is homogeneously distributed all around the dot with negligible projection into the molecule. The eigenvalues $\epsilon_{HOMO,\uparrow}$ and $\epsilon_{HOMO-1,\uparrow}$ are in the middle of the single-particle-HOMO−LUMO gap of the original quantum dot, with an energy splitting of 0.33 eV. The eigenvalue corresponding to the LUMO with spin down, $\epsilon_{LUMO,\downarrow}$, also represents a midgap level which is only 0.45 eV higher in energy than $\epsilon_{HOMO,\uparrow}$. Since $\psi_{HOMO,\uparrow}(\mathbf{r})$, $\psi_{HOMO-1,\uparrow}(\mathbf{r})$, and $\psi_{LUMO,\downarrow}(\mathbf{r})$ correspond to midgap levels, it is not surprising that they are spatially localized. Although $\psi_{HOMO-1,\uparrow}(\mathbf{r})$ and $\psi_{LUMO,\downarrow}(\mathbf{r})$ have the same orbital quantum number, their shape in real space is quite different because they have opposite spin; therefore, they experience a different exchange correlation potential in LSDA.

The stabilization of the intermediate state is due to three main factors: (1) the formation of an energetically favorable Si−C bond; (2) the reduction of the energy of the excited electron as it is localized at the stretched bonds around the reactant Si; and (3) finally the energy gain due to the exchange interaction between the electrons in the triplet state. As shown in Figure 1, the formation of a Si−C bond is necessary but not sufficient to stabilize an intermediate state. Factors 2 and 3 are in turn dependent on the exchange correlation functional used. Therefore, to make our results more robust, we repeated total energy calculations in the intermediate state geometry using an exchange correlation functional different from PBE, in particular B3LYP.

In the case of Si dots, B3LYP has been shown to give results for the energy gaps which are closer to quantum Monte Carlo values[27] than those obtained within PBE. Our results obtained within B3LYP show an enhancement of the effect observed within PBE. For instance, the distance from the reactant Si to

the core Si atoms is increased by 32% in B3LYP as compared with 10% in PBE, while the total energy of the singlet configuration is 0.85 eV (instead of 0.26 eV) higher than that of the triplet state. We think that the main reason for the difference between B3LYP and PBE results is the larger optical gap of the Si dot, obtained using the B3LYP approximation.

3.3.3. Transition-State Configuration. As expected, the *atomic configuration* of the intermediate state is not the lowest energy of the system in the triplet state ($S_z = 1$). The lowest energy of the ions is achieved when the H atom attached to the reactant Si is transferred to the second neighbor C, thus forcing a transition from an sp^2 to an sp^3 configuration and leaving all C and Si atoms 4-fold coordinated. It is interesting to note that the energy of the transition state [see Figure 2c] is slightly smaller than the sum of the energies of the relaxed dot and the detached molecule and much smaller than the energy required to excite the detached dot from the ground to the excited state [see Figure 2a]. Thus, provided that the energy transferred to the ions is not dissipated, the energy provided to the dot by the photon upon excitation is sufficient to overcome the reaction barrier and then reach the ionic minimum energy configuration [Figure 2d]. However, if the experimental conditions favor energy dissipation, then the intermediate triplet state would be available for detection.

At the transition point, the C−C distance increases to 1.49 Å, while, in the final configuration in the ground state, this distance is 1.55 Å. We note that, *after* the Si−C bond is formed and the reaction energy is dissipated, if the dot is excited from the singlet state, the energy provided by the photon is not sufficient to overcome the energy barrier required to break the Si−C bond. Therefore, the light activated process is irreversible.

The comparison between B3LYP and PBE suggests that the exciton energy gap has a strong influence on the intermediate state and the reaction path when the dot is excited to the triplet state. To clarify the influence of the exciton energy gap alone (within a given approximation for the exchange correlation energy) and to elucidate size effects, we performed calculations with a larger cluster ($Si_{66}H_{40}$). The surface of this cluster is also fully reconstructed (with only monohydrides in the (100) facets). To make a meaningful comparison, we choose one of the Si atoms in the (111) facets as the reactant Si. This reactant atom is identical in coordination up to the 3rd neighbor to the one chosen in $Si_{29}H_{24}$. Because the calculation of the transition energy barrier involves 318 degrees of freedom and 316 energy levels in PBE-LSDA, we assumed that the transition point has a coordination similar to the one found in $Si_{29}H_{24}$. We performed our calculations for the 66 Si atom cluster starting from configurations found for the 29 Si atom cluster, and we fully relaxed all the forces using the same accuracy as in the case of the smaller dot. As expected from quantum confinement effects, in both the reactant and product configurations, the energy difference between the triplet state and the singlet ground state decreases. For instance, the relaxed triplet state in $Si_{66}H_{39}$−CH_2−CH_3 is 1.81 eV above the ground state (compared to 2.17 in $Si_{29}H_{23}$−CH_2−CH_3). In the triplet state, the binding energy of the intermediate state is reduced to 0.47 eV (being 0.60 eV in the smaller cluster), while the energy barrier to cross the transition state from the intermediate state increases to 0.70 eV
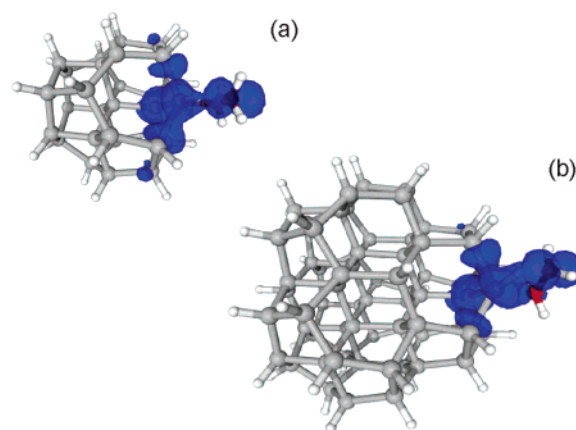
(27) Williamson, A. J.; Grossman, J. C.; Hood, R. Q.; Puzder, A.; Galli, G. *Phys Rev. Lett.* **2002**, *89*, 196803.

Figure 4. Comparison of the transition point spin densities in the triplet state ($S_z = 1$) corresponding to (a) $Si_{29}H_{24} + C_2H_4 \rightarrow Si_{29}H_{23}$−$CH_2$−$CH_3$ [see also Figure 2c] and (b) $Si_{66}H_{40} + C_2H_4 \rightarrow Si_{66}H_{39}$−$CH_2$−$CH_3$.

(as compared to 0.56 eV). Interestingly, the intermediate state energy measured with respect to the ground-state final configuration is very close to that of $Si_{29}H_{24}$ while the transition-state energy increases from 3.55 eV [see Figure 2c] to 3.69 eV. We also found that the intermediate state is stable in quantum dots as large as $Si_{142}H_{72}$ within the LDA.

As discussed above, the structural distortion and electronic distortions are highly localized around the reactant Si atom in the intermediate state. In the following, we demonstrate that similar localized distortions occur at the transition state.

In Figure 4, we compare the spin density of the triplet state at the transition point corresponding to (a) $Si_{29}H_{24} + C_2H_4 \rightarrow Si_{29}H_{23}$−$CH_2$−$CH_3$ [see also Figure 2c] and (b) $Si_{66}H_{40} + C_2H_4 \rightarrow Si_{66}H_{39}$−$CH_2$−$CH_3$. We see that, besides minor differences in the atomic positions and in the spin density, the two configurations are very similar. One important point is that most of the spin density is localized around the reactant Si. This property suggests that the energy of the configuration depends essentially on the local structure and not on the size of the quantum dot. In addition, it suggests that the higher energy of the transition in the larger dot might be related to a different pre-existing strain at the surface due to dimer reconstructions. Similar observations can be made if we compare the intermediate-state spin density of $Si_{66}H_{40} + C_2H_4$ (not shown) with the one of Figure 3. Because of the localized nature of the single particle states and spin density associated with the triplet state ($S_z = 1$), the energy of the transition state and that of the intermediate state should depend weakly on size. In contrast, the spin densities of both the reactant and the product are distributed over the entire Si cluster, and this is consistent with quantum confinement effects. As a consequence, the reactant and product energies do depend on size. This implies that, in the excited state, barriers increase and binding energies decrease as the quantum dot becomes larger. This is consistent with the experimental fact that white-light-activated reactions are only observed in porous Si and not in flat bulk surfaces[2] where they are only possible under UV light. Our interpretation of the experimental observation is the following: the energy provided by the excitation is used to overcome the barriers in the excited state, and smaller energy gaps induce smaller changes in the barriers.

3.3.4. Discussion of Experimental Findings. Recently Stewart and Buriak[2] suggested a mechanism for the light-

activated hydrosilylation reaction that consists of the transfer of a hole to the alkene followed by the formation of a Si−C bond and, subsequently, a transfer of the electron from the dot to an H atom, followed by H migration. This intuitive picture is in qualitative accord with the results of our simulation: indeed we find that a Si−C bond forms first in the intermediate state, and then there is a partial transfer of a positive charge to the molecule. In our results, this is reflected in the formation of a dipole moment pointing to the C_2H_4 molecule as it approaches the dot. This calculated dipole moment is reversed when the molecule is chemically attached to the dot, due to the formation of a polar Si−C bond. However, we find some differences with respect to the mechanism proposed in ref 2: (1) The concept of an electron−hole pair is not really a good description of the electronic state at the intermediate and at the transition-state configurations as explained in section 3.3.2. (2) The electron is never transferred to the hydrogen atom, and (3) the triplet exciton "returns" to the dot when the reaction is completed, which is visualized as the spin density is homogeneously distributed in the dot. Thus, provided that it does not decay, the exciton could act as a catalyst for more than a single reaction.

3.4. Other Unsaturated Chains. The results obtained here for three different sizes suggest that an intermediate state would form as long as the exciton gap is larger than the intermediate-state formation energy. The behavior of the spin density in Figure 3a strongly suggests that the double bond nature of the ethene molecule plays a crucial role in the formation of the intermediate state. Therefore, other double bonded or triple bonded molecules could form a similar intermediate bound state when the dot is excited in the triplet state. To address this issue, we repeated some of our calculations with the ethyne molecule. We find that ethyne also forms an intermediate bound state with a binding energy of about 0.81 eV (which is larger by 0.2 eV than the one obtained with C_2H_4). However, to reach this intermediate state, the ethyne molecule has to overcome a barrier of 0.07 eV. This small energy barrier is required in order to change the sp hybridization of the C atoms to sp^2. However, this barrier is still smaller than the Stokes-shift relaxation energy for this cluster ($\sim$0.45 eV). Thus the reactions involving alkynes could also be catalyzed by light by the same mechanism proposed here for alkenes.

4. Conclusions and Remarks

We have provided a theoretical description of the experimentally observed[2] light activated functionalization of porous Si with unsaturated hydrocarbons. We found that, in the presence of light, the energy barriers for the reaction are drastically reduced. The reduction of the activation energies is related to the exciton gap which determines the relative position of the initial and final states energies as compared to the transition point. Therefore, excited-state energy barriers increase as the gap of the dot decreases. Our results indicate that the reaction energy path in the excited state leads to a metastable, spin-polarized state that, in principle, could be measured in, for example, electron spin resonance experiments.

We note than even after size selection is achieved experimentally, an ensemble of quantum dots will present some dispersion in the values of their optical gaps. Indeed, Si dots with an identical number of atoms may have different surface structures, and the optical gap of a Si QD is very sensitive to surface reconstructions and defects,[20] as well as to surface passivants.[28] Our results for hydrosilylation reactions in the excited state suggest a way to "gap" select Si dots: (i) An ensemble of dots exposed to monochromatic light will be split into two sets with quite different chemical reactivities. The ones with gaps smaller than the energy of the incoming photons will be excited and will react very efficiently with unsaturated hydrocarbons. On the other hand, the dots with gaps larger than the incoming light will remain essentially inert as compared with the excited ones, since the reaction rate will be damped by the exponential $\exp(-E_B/k_BT)$, where E_B is the energy barrier ($\sim$2 eV) and k_BT is the thermal energy. (ii) Among the excited dots, the ones with larger gaps will tend to react faster because energy barriers increase and binding energies decrease as the gap of the dot becomes smaller. (iii) Very large dots will not be significantly affected by photoactivation, which is consistent with the experimental fact that this type of effect is uniquely related to quantum confinement.[2] Considering factors i and ii, we propose to gradually increase the energy of the incoming photons starting from the onset of the absorption spectra of the incoming light (a standard florescence line narrowing technique[29]). By doing so, the dots with the lowest-energy gap (which we refer to as group I dots) will be excited first. Once these chemically active, excited dots of group I are fully functionalized with a given chemical A, the energy of the incoming photons can be increased, and a new group of dots (group II) will be excited. At this point, the dots of group I, although electronically and thermally excited by the incoming light, are chemically inert since they have no accessible Si−H bonds and the hydrosilylation reaction is irreversible. Therefore, if a new chemical B is injected into the system, this will react only with group II dots, which will then be functionalized in a different manner with respect to those of group I. Once functionalization of group II is completed, the incoming energy can be further increased and the process repeated until all dots are functionalized. Accordingly, different molecules could be associated directly with the photoluminescence energy, without requiring a physical separation of the dots. In addition, only the dots that have long exciton lifetimes and are free of defects inducing nonradiative decays would be functionalized.

(28) Puzder, A.; Williamson, A. J.; Grossman, J. C.; Galli, G. *Phys. Rev. Lett.* **2002**, *88*, 097401.
(29) Nozik, A. J.; Mićić, O. I. *MRS Bull.* **1998**, *23*, 24−30.